



# Study the Optimal Control of VSC-HVDC System for Improved Controller Performance

Nadam Lavudya

Assistant Professor, Brilliant Group of Institutions, Ranga Reddy, Telangana India.  
lavudyanadam@gmail.com

**Abstract:** - In this study, optimal control of voltage source converter- high voltage direct current (VSC-HVDC) transmission systems is modeled and its performance in weak networks is compared with strong systems. The comparison is made considering how they track the desired values of DC voltage and AC current while switching or fault occurs, which determines the system stability. A proportional-integral controller with decoupled control variables of a typical generator-load VSC-HVDC system is proposed for optimal control. Simulation results show that a fault caused by switching in weaker networks, of which the short circuit level is lower rather than stable networks, leads to higher changes in DC voltage and AC current.

**Keywords:** VSC, HVDC, Pi, Controller, loop, DC, AC

## I. INTRODUCTION

The recent developments in the power delivery are influenced by the progress of conventional power production, which mainly use primary energy resources that are limited and cause environmental problems. The technology of high voltage direct current (HVDC) transmission can be a solution to this problem [1-2]. Supporters of the HVDC technology contend that it has environmental and economical benefits as follows [3]

- Transferring larger amounts of energy, especially in under-sea transmission. DC systems, as opposed to long AC systems, are free of the cable capacitance that limits the possible transmission distance.
- Reducing active power losses as HVDC has lower transmission losses than AC system, even regarding converter losses.
- Connecting asynchronous systems, particularly systems with different nominal frequencies.
- Controlling all DC and AC parameters with acceptable accuracy and speed. Moreover, constant power can be transferred and fluctuations would be rather damped contrary to AC network.
- Decreasing short circuit currents. HVDC systems, unlike AC systems, do not contribute to short circuit currents.

The configuration of HVDC network is determined according to the mode of converter and location of conversion stations. The main configurations are [3]:

- Point to point HVDC transmission: uses overhead lines or submarine cables to connect to converter stations. The ground is used as a return path.

- Back to back HVDC stations: the two converters are located in the same station and are used to connect two asynchronous AC systems.
- Multi-terminal HVDC system: more than two converter stations are included.

Therefore, HVDC systems have drawn a lot of attention because of their advantages over HVAC transmission, including environmental, technical and economical merits. Weak networks have lower short circuit level and a relatively high electrical impedance but less inductance to impedance ratio in comparison with strong systems. HVDC converters connected to weak AC networks suffer from stability problems due to adverse DC-AC system interactions. Voltage source converter- high voltage DC (VSC-HVDC) systems feature independent active and reactive power regulation and black start capability and can provide connection between weak AC networks, in contrast to conventional thyristor-based HVDC transmission. Although one of the original purposes for the use of VSC- HVDC systems was the possibility to connect to very weak AC systems, some difficulties have been experienced. [4-7]

Some transmission systems use the line commutated converter (LCC) based on current source converter (CSC) through thyristor technology. The problem with this method is that thyristor turn off is not controlled with gate signal. [8] Owing to the development of power electronics, voltage source converter (VSC) has become more practical. At first, VSC-HVDC was invented by B. T. Ooi and X. Wang in 1990. [9] It uses self-commutating switches, which are gate-turn-off thyristors (GTOs) and insulated gate bipolar transistors (IGBTs) that can be either turned on or off. Power electronics developments has given rise to HVDC Light, based on Pulse Width Modulation to produce voltage, independent of AC. Siemens has offered VSC-HVDC variant, commercialized as HVDC Plus, which uses a multi-level approach. The first commercial VSC based HVDC transmission was commissioned in 1999

on Gotland Island with an underground cable of 50 km. The topologies of VSCs to increase the transferred power are classified into three types including: two levels converter, three levels converter and modular multilevel converter. The evolution of power electronics has led to progress of control techniques to improve VSC-HVDC systems' stability. The design of controllers for VSC-HVDC system is mainly based on mathematical models.

However, the system will be influenced by the external uncertainties, such as the stochastic fluctuation of the

faults in AC system and DC link. Hence, it is necessary to improve the VSC-HVDC transient stability and to reduce the influences of uncertainties. In this way, many linear and nonlinear control strategies of VSC-HVDC systems have been developed, including proportional-integral (PI) [10, 11] control scheme. [8, 12] Conventional PI

controllers, based on inner and outer control loops, are being widely studied. Modeling and optimal control of GL (generator-load) VSC-HVDC transmission systems in order to enhance system stability is designed in [13].

This study aims to compare transient stability of weak networks with strong systems. The optimal PI controller is simulated using MATLAB/Simulink and tracking the desired values of DC voltage and AC current while switching or faults occurs, is investigated regarding time constant and fault correction.

## II. MODELING VSC-HVDC SYSTEMS

The typical system consists of a converter substation of the HVDC transmission system on DC side and AC network with impedance  $Rl+jLl$ . Capacitor  $C1$  in the DC side boosts the DC voltage in order to feed load ( $R+jL$ ).

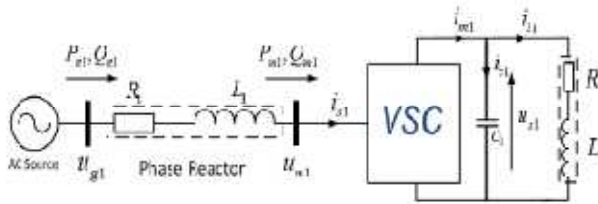


Figure 1: Basic Structure of GL VSC-HVDC.

Figure 1 illustrates the structure of studied system. As can be seen, it consists of AC network and DC side connected through a converter in rectifier mode. Applying the Kirchhoff's theorem for the voltages in the AC side gives

$$L_1 \frac{di_{s1}}{dt} + R_1 i_{s1} = u_{g1} - u_{m1} \quad (1)$$

The voltage drop in each phase is depicted by Eq. (1). The balanced three-phase system is defined in  $d-q$  reference by

$$\vec{u}_{g1} = u_{g1d} + j u_{g1q} \quad (2)$$

$$\vec{u}_{m1} = u_{m1d} + j u_{m1q} \quad (3)$$

$$\vec{i}_{s1} = i_{s1d} + j i_{s1q} \quad (4)$$

Moreover,

$$\vec{u}_{m1} = m_{1d} \frac{u_{s1}}{2} + j m_{1q} \frac{u_{s1}}{2} \quad (5)$$

$$m_{1d} = 2 \frac{u_{m1d}}{u_{s1}}, \quad m_{1q} = 2 \frac{u_{m1q}}{u_{s1}} \quad (6)$$

where  $m_{1d}$  and  $m_{1q}$  are the dimensionless  $d-q$  components that depict the relation between the  $d-q$  voltage on the AC side of the VSC-HVDC transmission system and the DC bus voltage  $u_{s1}$ .

$$P_m = \frac{3}{2} (u_{m1d} i_{s1d} + u_{m1q} i_{s1q}) \quad (7)$$

Thus, by applying the power equality constraint on both sides of the rectifier

$$P_{m1c} = P_{mDC} \Rightarrow u_{s1} i_{m1} = \frac{3}{2} (u_{m1d} i_{s1d} + u_{m1q} i_{s1q}) \quad (8)$$

Considering Eqs. (1), (6) and (8), the continuous-time mathematical model of VSC-HVDC system that specifies the different relations amongst the circuit components, is indicated by the following state space equations:

$$\begin{cases} \frac{di_{s1d}}{dt} = -\frac{R_1}{L_1} i_{s1d} + \omega i_{s1q} - \frac{1}{2L_1} m_{1d} u_{s1} + \frac{1}{L_1} u_{g1d} \\ \frac{di_{s1q}}{dt} = -\omega i_{s1d} - \frac{R_1}{L_1} i_{s1q} - \frac{1}{2L_1} m_{1q} u_{s1} + \frac{1}{L_1} u_{g1q} \\ \frac{du_{s1}}{dt} = \frac{3}{4C_1} m_{1d} i_{s1d} - \frac{3}{4C_1} m_{1q} i_{s1q} - \frac{1}{C_1} i_{L1} \\ \frac{di_{L1}}{dt} = \frac{1}{L} u_{s1} - \frac{R}{L} i_{L1} \end{cases} \quad (9)$$

The active and reactive powers, applied to AC side at the beginning and the end of AC line, are given by  $P_{g1}$ ,  $Q_{g1}$ ,  $P_{m1}$  and  $Q_{m1}$ , respectively:

$$\begin{cases} P_{g1} = \frac{3}{2} (u_{g1d} i_{s1d} + u_{g1q} i_{s1q}) \\ Q_{g1} = \frac{3}{2} (u_{g1q} i_{s1d} - u_{g1d} i_{s1q}) \\ P_{m1} = \frac{3}{2} (u_{m1d} i_{s1d} + u_{m1q} i_{s1q}) \\ Q_{m1} = \frac{3}{2} (u_{m1q} i_{s1d} - u_{m1d} i_{s1q}) \end{cases} \quad (10)$$

## III. OPTIMAL CONTROL FOR VSC-HVDC

### A. Control Problem Formulation

After modeling the steady state, it is necessary to maintain unity power factors in AC side of the VSC-HVDC and govern the DC voltage. Hence, the control system, based on inner current control loop, controls the AC current and outer controllers supply the DC voltage to the desired values. For this purpose, optimal PI controllers are proposed to control the voltage on the VSC's AC side and the DC current. The optimal PI controller is given by the following transfer function:

$$PI_i(s) = \frac{v}{e} = k_{pi} + \frac{k_{ii}}{s} \quad (11)$$

where  $v$  and  $e$  refer to the output of the controller and the error between the reference and the under control state variable, respectively. The dynamics of the error can be written in the state space by:



# International Journal of Ethics in Engineering & Management Education

Website: www.ijee.in (ISSN: 2348-4748, Volume 4, Issue 9, September 2017)

$$x_e^{\square} = A_e x_e + B_e v_i \text{ where } x_e = \begin{bmatrix} e_i \\ z_i \end{bmatrix}$$

The optimal parameters are obtained by minimizing a quadratic criteria  $J$ , as follows:

$$J = \frac{1}{2} \int_0^{+\infty} (x_e^T Q x_e + v_i^T R v_i) dt \quad (13)$$

The state equation of Eq. (12) with the criterion given by Eq. (13) generate

$$v_i = -K_i x_e \quad (14)$$

Where

$$K_i = R^{-1} B_e^T S_i \quad (15)$$

$S$  is a symmetric non-negative matrix that is the solution of the Riccati equation

$$S_i A_e + A_e^T S_i - S_i B_e R^{-1} B_e^T S_i + Q = 0 \quad (16)$$

By using LQR from MATLAB, we will gain:

$$K_i = [k_{pi}, k_{ii}] \quad (17)$$

## B. Optimal PI Controller

A method of VSC-HVDC control via  $PI$  controllers is studied. Based on this model, two control loops are obtained that have two controllers  $PI1$  and  $PI2$ . The inner loop regulates the AC currents  $is1d$  and  $is1q$  and the outer loop controls the voltage  $us1$  in the DC side.

### B.1. Inner current control loop

From Eq. (9), the variations of the AC current can be expressed by

$$\begin{cases} \frac{di_{s1d}}{dt} = -\frac{R_1}{L_1} i_{s1d} + \frac{1}{L_1} u_{1d} \\ \frac{di_{s1q}}{dt} = -\frac{R_1}{L_1} i_{s1q} + \frac{1}{L_1} u_{1q} \end{cases} \quad (18)$$

Where

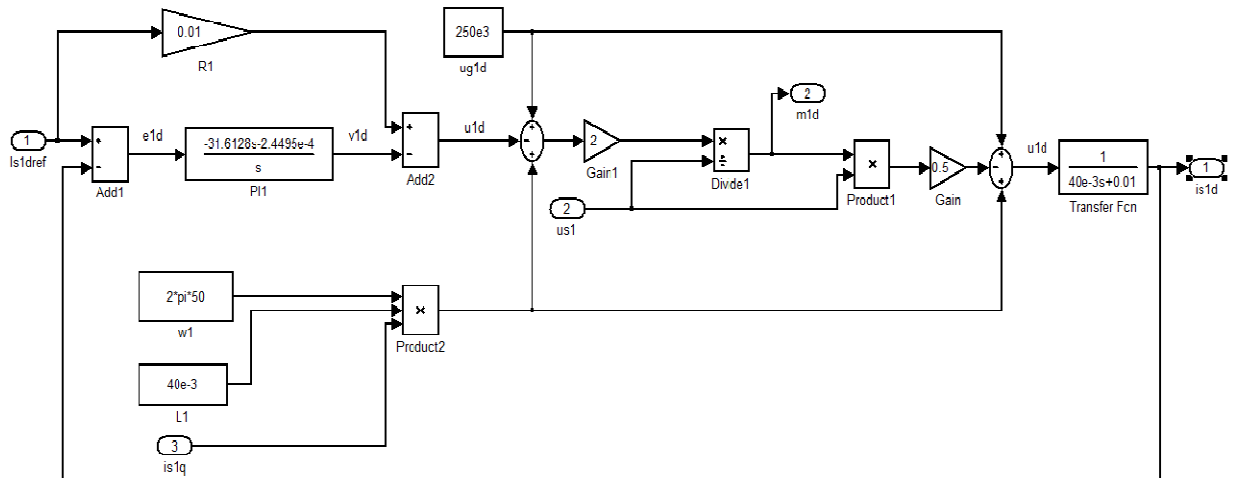


Figure 2: Outer Control Loop for AC Current  $is1d$ .

$$\begin{cases} u_{1d} = \omega_1 L_1 i_{s1q} - \frac{1}{2} m_{1d} u_{s1} + u_{s1d} \\ u_{1q} = -\omega_1 L_1 i_{s1d} - \frac{1}{2} m_{1q} u_{s1} + u_{s1q} \end{cases} \quad (19)$$

Substituting  $is1d$  and  $is1q$  respectively, by  $(Is1dref - e1d)$  and  $(Is1qref - e1q)$  in Eq. (18), the variations of the errors  $e1d$  and  $e1q$  and their integrals named  $z1d$  and  $z1q$  are expressed by

$$\begin{cases} \frac{de_{1d}}{dt} = -\frac{R_1}{L_1} e_{1d} + \frac{1}{L_1} v_{1d} \\ \frac{dz_{1d}}{dt} = e_{1d} \\ \frac{de_{1q}}{dt} = -\frac{R_1}{L_1} e_{1q} + \frac{1}{L_1} v_{1q} \\ \frac{dz_{1q}}{dt} = e_{1q} \end{cases} \quad (20)$$

where the outputs of the  $PI1$  controllers are given by

$$v_{1d} = R_1 I_{s1dref} - u_{1d}$$

$$v_{1q} = R_1 I_{s1qref} - u_{1q}$$

So, the control signals are

$$\begin{cases} m_{1d} = \frac{2}{u_{s1}} (-u_{1d} + \omega_1 L_1 i_{s1q} + u_{s1d}) \\ m_{1q} = \frac{2}{u_{s1}} (-u_{1q} - \omega_1 L_1 i_{s1d} + u_{s1q}) \end{cases} \quad (22)$$

According to the proposed optimal approach and the decoupling control method, the current  $is1d$  control loop is illustrated in Figure 2.

The gains of the inner current control loops are obtained from the proposed optimal control approach, which guarantees fast operation of the inner loop with the desired settling time.

### B.2. Outer control loop

From Eq. (9), the variation of the DC voltage can be specified as

$$\frac{du_{s1}}{dt} = \frac{1}{C_1} i_{c1} \quad (23)$$

where, the output of the optimal PI2 controller is

$$i_{c1} = \frac{3}{4} m_{1d} i_{s1d} + \frac{3}{4} m_{1q} i_{s1q} - i_{L1} \quad (24)$$

Substituting  $us1$  by  $(Us1ref - e1c)$  into (23), the variations of the error  $e1c$  and its integral  $z1c$  would be

$$\begin{cases} \frac{de_{1c}}{dt} = -\frac{1}{C_1} i_{c1} \\ \frac{dz_{1c}}{dt} = e_{1c} \end{cases} \quad (25)$$

According to the state-space equations given by Eq. (25), the minimization of the quadratic criterion  $J$  results in the stability

of the GL VSC-HVDC system. Hence, from Eq. (24), we obtain

$$I_{s1dref} = \frac{4}{3m_{1d}} (-i_{c1} - 0.75m_{1q}i_{s1q} + i_{L1}) \quad (26)$$

Consider that we can divide by  $m1d$  because this control variable would never become zero. Furthermore, the reactive power would be controlled through the current  $is1q$  as follows [13]

$$I_{s1qref} = \frac{\frac{3}{2} u_{m1q} i_{s1d} - Q_{m1ref}}{\frac{3}{2} u_{m1d}} \quad (27)$$

The outer control loop is depicted in Figure 3. The gains of PI2 controller are also determined by the optimal approach, which guarantees a slower dynamic of the outer loop in the desired settling time. The outer loop controls the reactive power and the DC voltage.

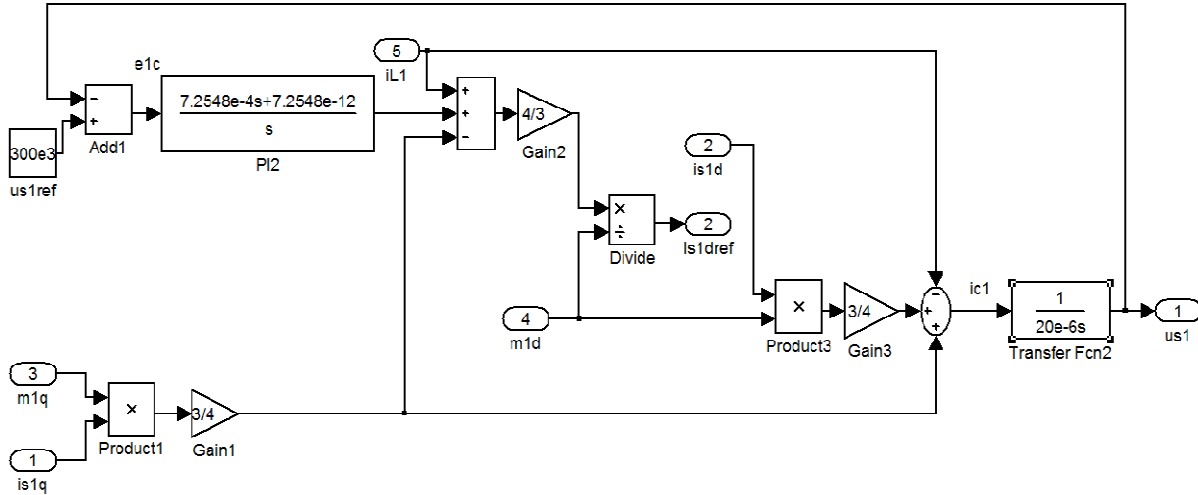


Figure 3: Outer Control Loop for DC Voltage  $us1$

## IV. SIMULATION

To verify the validity of the proposed control strategies and to survey the problems with the weak networks rather than typical strong systems, simulation studies of the VSC-HVDC system are undertaken via MATLAB/SIMULIK in the operating conditions.

### A. System Parameters

The parameters of VSC-HVDC transmission system and the optimal PI controllers' coefficients, which are obtained through LQR method are listed respectively in Tables 1, 2 and 3.

Table 1: Parameters of the Simulation System.

Frequency of AC network (Hz)	50
AC line resistor R1 ( $\Omega$ )	0.01
AC line reactor L1 (mH)	40
Shunt capacitors C1 ( $\mu$ F)	20
Load resistance R ( $\Omega$ )	450
Load inductance L (mH)	11.5
Input voltage $ug1d$ (kV)	250
Input voltage $ug1q$ (V)	0
Rated DC Voltage $us1$ (kV)	300



Table 2: Gain of Optimal *PI* Controller in a Strong System.

$k_{pi}$	Values	$k_{ii}$	Values
$k_{p1}$	-31.6128	$k_{i1}$	$-2.4495 \times 10^{-4}$
$k_{p2}$	$7.2548 \times 10^{-4}$	$k_{i2}$	$7.2548 \times 10^{-12}$

Table 3: Gain of Optimal *PI* Controller in a Weak Network.

$k_{pi}$	Values	$k_{ii}$	Values
$k_{p1}$	-31.5928	$k_{i1}$	$-2.4479 \times 10^{-4}$
$k_{p2}$	$7.2548 \times 10^{-4}$	$k_{i2}$	$7.2548 \times 10^{-12}$

**B. Simulation Results**

The behavior of the system outputs, while a change occurs in the load current *ill* due to switching in the weak and strong power systems have been studied. Using these optimal gains, DC voltage *Us1* and *Q1* are controlled in order to track their reference values, 300KV and 0, respectively. Current *is1d* behavior in strong and weak networks during two switching is shown in Figures 4 and 5 and the behavior of DC voltage (*Us1*) in the two different conditions is shown in Figures 6 and 7. As can be seen, in both conditions, the optimal *PI*

controllers behave efficiently to decrease the fluctuations of DC voltage and AC current and improve the stability of the VSC-HVDC system. The time responses of DC voltage and AC current reach to a new stable steady-state value in response to load changes. However, in weak networks that the short circuit level is rather low, any kind of fault such as switching cause more changes in DC voltage and AC current. *Is1q* had a similar behavior in both conditions and was near zero as it was expected.

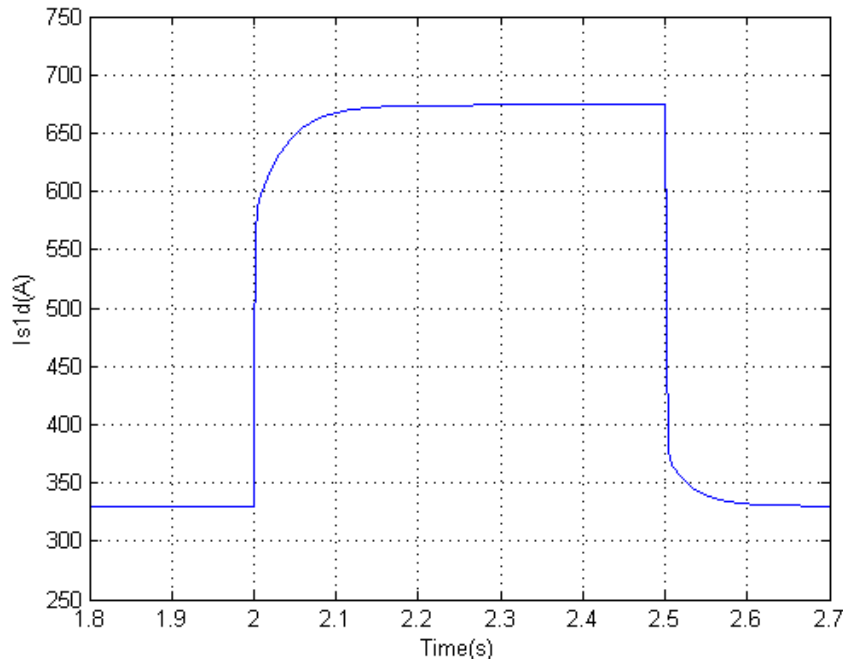


Figure 4: Current *is1d* Behavior in a Strong Power System.

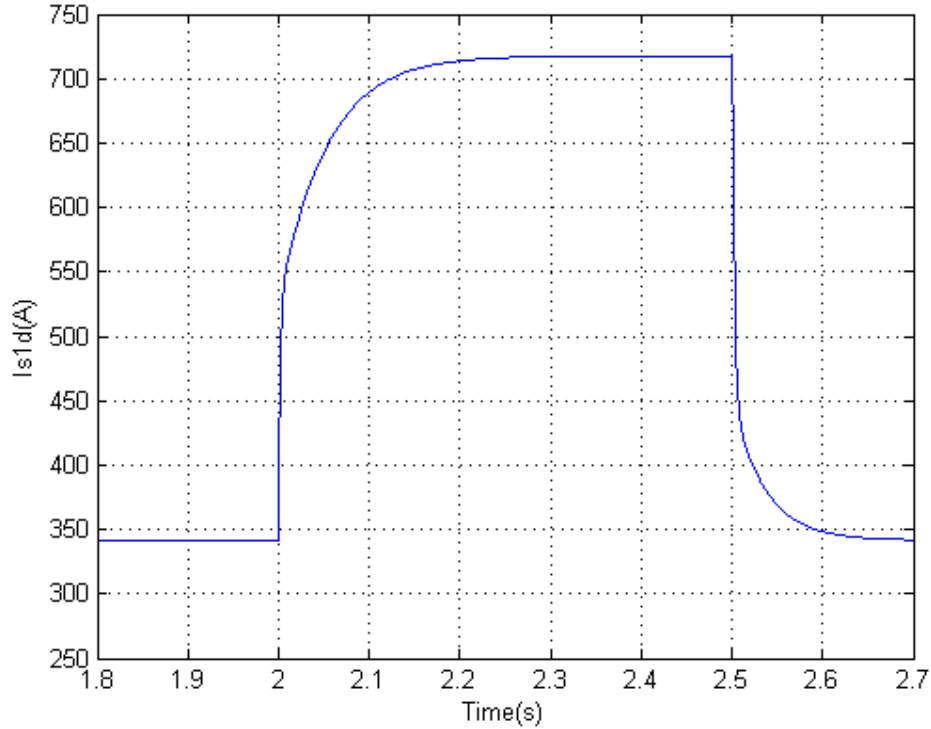


Figure 5: Current  $i_{s1d}$  Behavior in a Weak Network.

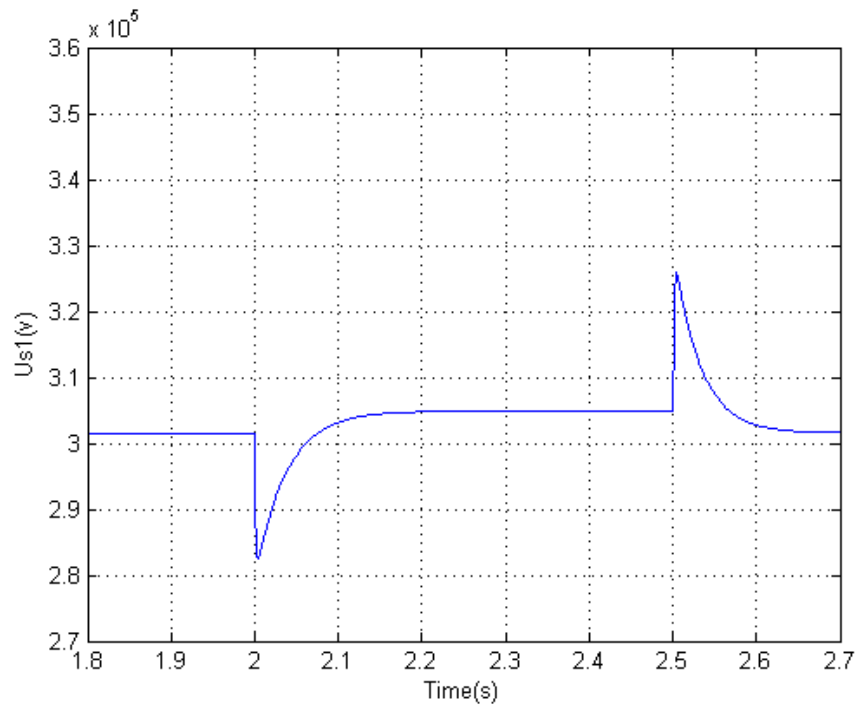


Figure 6: Voltage  $u_{s1}$  Behavior in a Strong Power System.

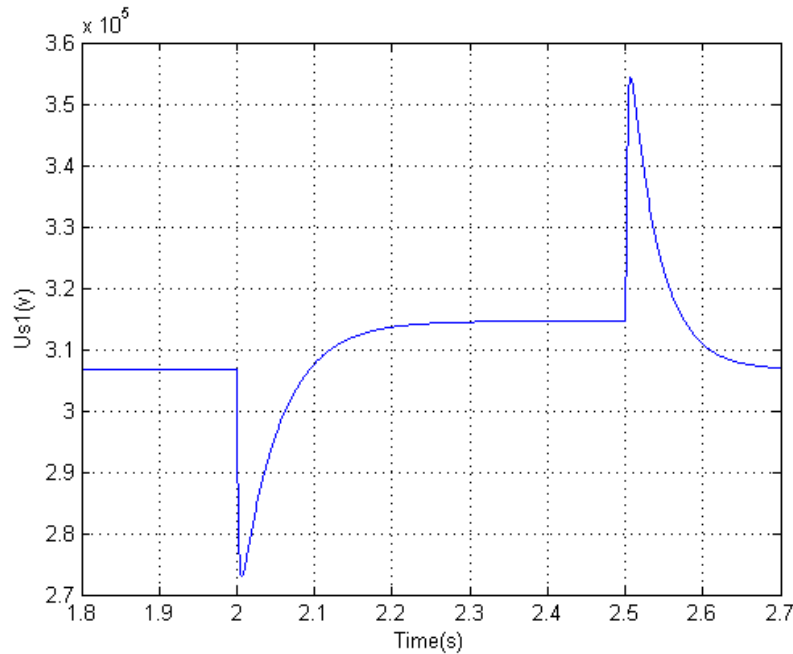


Figure 7: Voltage  $us1$  Behavior in a Weak Network.

## V. CONCLUSIONS

It is necessary to design efficient control strategies to satisfy stability of VSC-HVDC transmission systems under the external changes and different situations. After developing the mathematical model of the system, an optimal control method is designed and formulated to govern the DC link voltage and to control the reactive power in AC side of the VSCHVDC system. The PI controllers, which work through two faster inner loops to control AC current and a slower outer loop to maintain DC voltage and the reactive power, are designed to improve the system performance. The gains of PI controllers are calculated using the optimal LQR method. To prove the efficiency of the proposed control strategy, with aim to study its performance in weak networks, the system is simulated via Matlab/Simulink in operating conditions. It is determined from the results that faults in weak networks cause more changes and takes more time to improve, as compared to the strong systems.

## REFERENCES

- [1]. N. Barberis Negra, J. Todorovic, and T. Ackermann. (2006). Loss evaluation of HVAC and HVDC transmission solutions for large offshore wind farms. *Electric Power Systems Research, Elsevier*, Vol. 76, 916-927.
- [2]. I. M. de Algeria, J. L. Martin, I. Kortabarria, J. Andreu and P. I. Ereno. (2009). Transmission alternatives for offshore electrical power. *Renewable and Sustainable Energy Reviews, Elsevier*, Vol. 13, 1027-1038.
- [3]. H. S. Ramadan, H. Siguerdidjane, M. Petit, R. Kaczmarek. (2012). Performance enhancement and robustness assessment of VSC HVDC transmission systems controllers under uncertainties. *International Journal of Electrical Power & Energy System, Elsevier*. 34-46.
- [4]. Sharma, R. Rasmussen, T.W. Jensen, K.H. Akamatov, V. (2010). Modular VSC converter based HVDC power transmission from offshore wind power plant: Compared to the conventional HVAC system. *Electric Power and Energy Conference (EPEC), IEEE*, (pp. 1-6). Halifax, NS.
- [5]. Eghlimi, M. Shakouri, G.H. (2008). Economic analysis of Iran-Turkey power network interconnection: HVDC vs. HVAC, *IEEE 2nd International Power and Energy Conference*, 164 - 168. Johor Bahru.
- [6]. Beccuti, G. Papafotiou, G. Harnefors, L. (2014). Multivariable Optimal Control of HVDC Transmission Links With Network Parameter Estimation for Weak Grids. *The International Journal of Control Systems Technology, IEEE Transactions*, Vol. 22, 676 - 689.
- [7]. O'Reilly, J. Wood, A.R. Osaukas, C.M. (2003). Frequency domain based control design for an HVDC converter connected to a weak AC network. *IEEE Transactions on Power Delivery*, Vol. 18, 1028 - 1033.
- [8]. Si-Ye. Ruan, Guo-Jie. Li, Lin. Peng, Yuan-Zhang. Sun and T.T. Lie. (2007). A nonlinear control for enhancing HVDC light transmission system stability. *International Journal of Electrical Power & Energy Systems*, Vol. 29, 565-570.
- [9]. M. Yin, G. Li, M. Zhou and C. Zhao. (2008). Simplified Input-Output linearization control for windfarm interconnection based on multi-terminal VSC-HVDC. *16<sup>th</sup> PSCC*, (pp. 1-7). Glasgow, Scotland.
- [10]. V. Blasko and V. Kaura. (1997). A new mathematical model and control of a threephase AC-DC voltage source converter, *IEEE Transactions on Power Electronics*, Vol. 12, 116-123.
- [11]. C. Bajracharya, M. Molinas, Y.A. Suul and T.M. Undeland. (2008). Understanding of tuning techniques of converter controllers for VSC-HVDC. *Nordic Workshop on Power and Industrial Electronics*, pp 1-8.
- [12]. Si-Ye. Ruan, Guo-Jie. Li, X. H. Jiao, Yuan-Zhang. Sun and T.T. Lie. (2007). Adaptive control design for VSC-HVDC systems based on backstepping method. *Electric Power Systems Research, Elsevier*, Vol. 77, pp. 559-565.
- [13]. Mohamed Ayari, Mohamed Moez Belhaouane, Naceur Benhadj raiek, Xavier Guillaud. (2013). Optimal Control Design for VSC-HVDC Systems. *IEEE International Conference on Electrical Engineering and Software Applications (ICEESA)*, (pp. 1-6). Hammamet.